# Calculation of MnO Activity in Aluminate Slags at Various Temperatures

L. Erfani[1], E. Keshavarz Alamdari[2]* and Y. Ganjkhanloo[3]

[1] *Ceramic Department, Materials and Energy Research Center (MERC), P.O. Box 14155-4777, Tehran, Iran.*

[2] *Department of Mining and Metallurgical Engineering, Amirkabir University of Technology, P.O. Box 15875-4413, Tehran, Iran.*

[2,3] *Research Center for Materials and Mining Industries Technology, Amirkabir University of Technology, P.O. Box 15875-4413, Tehran, Iran.*

## Abstract

In this research, the activity of MnO, produced during steel making in aluminate-rich slags, was investigated. According to thermodynamic equations and mathematical calculation, a series of relations was obtained for evaluation of oxide activity using Masson's theory. The obtained relations were solved according to Levenberg-Marquardt method and using Matlab software. The results were correlated with the experimental Data. To derive relations, it was assumed that the solution has ideal behavior and the polymeric chains are linear. Finally, a relation was derived for oxide activity calculation which can be used in a wide range of concentration. MnO activity was investigated at various temperatures, using the experimental data and the obtained relation. Furthermore, the relation between equilibrium constant (K) and temperature was obtained. By means of the results the viscosity of melt can also be forecasted.

*Keywords:* Oxide activity, Masson's theory, MnO.

## 1. Introduction

Slags are one of the important parts of steel making industry; therefore the study of physicochemical behavior of slags is very fundamental. Slags are the ionic liquids which various theories have been presented to determination of slags constitution activity. For this purpose, one of the most prominent theories is Masson's theory that it was extended for silicate slags.

The prediction of slags properties for production of the pure molten metal and interpreting the physicochemical behavior of slag is very promising. Therefore, estimation of constituent activity in the slag is essential. The theories concerned with slags can be divided into two main groups: molecular theory and ionic theory. Conventionally, the intricate anionic complex was formed in acidic slags. The ionic theories usually are used for alkaline slags. The well-known ionic theories of slags are Temkin's theory, Flood's Theory and Masson's Theory [1,2].

Masson's theory has been employed for alkaline oxide activity calculation in silicate slags with complex anions. This type of slags contains complex silicate polymers. Strong alkaline slags usually have $SiO_4^{4-}$ ions while the weaker ones have ions such as $SiO_4^{4-}$, $Si_2O_7^{6-}$ etc. Equilibriums related to ionic polymers of silicate complexes have been shown in equation (1-3) as following [1,3]:

$$SiO_4^{4-} + SiO_4^{4-} = Si_2O_7^{6-} + O^{2-} \quad (1)$$

$$SiO_4^{4-} + Si_2O_8^{6-} = Si_3O_{10}^{8-} + O^{2-} \quad (2)$$

$$SiO_4^{4-} + Si_3O_{10}^{8-} = Si_4O_{12}^{10-} + O^{2-}, ect. \quad (3)$$

According to Temkin's theory, the activity of oxide in the ionic solution can be calculated by the equation (4) [4,5]:

$$a_{MO} = X_{M^{+2}} . X_{O^{-2}} \quad (4)$$

If $X_{M^{+2}} = 1$ then $a_{MO} = X_{O^{-2}}$.

Assuming solutions as ideal and equilibrium constant (k) as invariable, the following relation can be derived on the basis of $SiO_2$ activity in order to calculation of MO activity [6].

$$\frac{1}{x_{SiO_2}} = 2 + \frac{1}{1-a_{MO}} - \frac{3}{1-a_{MO}+3a_{MO}/K_1} \quad (5)$$

In the above relation, the $X_{SiO_2}$ denotes the mole fraction of silicate ion. For linear chains, the above equation can be reformed as equation (6):

$$\frac{1}{x_{SiO_2}} = 3 - K_1 + \frac{a_{MO}}{1-a_{MO}} - \frac{K_1(K_1-1)}{K_1 + \frac{a_{MO}}{1-a_{MO}}} \quad (6)$$

* *Corresponding author:*
*Tel: +98 21 645 42971* *Fax: +98 21 664 05846*
*Email: alamdari@aut.ac.ir*
*Address: Department of Mining and Metallurgical Engineering, Amirkabir University of Technology, P.O. Box 15875-4413, Tehran, Iran.*
*1. M.Sc.*
*2. Associate Professor*
*3. M.Sc.*

It can be plotted acticity curve using these equation for various oxides such as CaO, PbO, MnO, FeO and SnO. For this purpose, a value for $K_1$ should firstly be selected; then using equation (6), the curve of activity versus silicate mole fraction can be plotted (Figure 1). This curve has the fine accuracy at high temperatures and in $\Delta G_{mix}$<-12kcal [7,8].

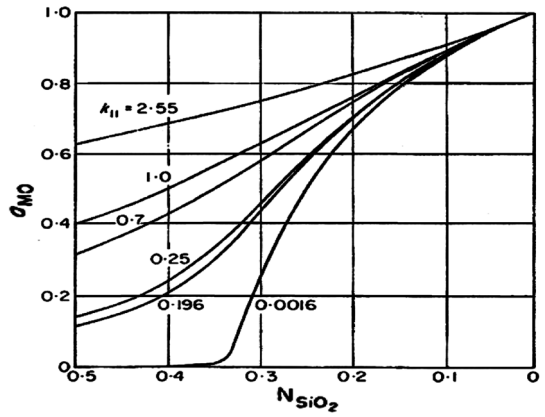


*Fig. 1. Diagrams of theorical activity of MO in binary mixtures; from up to down CaO, PbO, MnO, FeO and SnO [4].*

## 2. Methods

This study was exerted based on mass conservation law in slag system. According to the equilibrium ratios of reactions (K), besides the mass equilibrium of components, a multi component equation was formed. This equation was solved according to Levenberg–Marquardt's analytical method and utilizing Matlab software [9]. Eventually, it was computed the activity of MnO for various $Al_2O_3$ at different values of K.

## 3. Results and Discussion

Ionization and polymerization equations of Alumina are the basis of mass equations.
Ionization equations of alumina are as following:

$$Al_2O_3 = A1^{3+} + AlO_3^{3-} \quad (7)$$

$$AlO_3^{3-} + AlO_3^{3-} = Al_2O_5^{4-} + O^{2-} \qquad K_{11} \quad (8)$$

$$Al_2O_5^{4-} + AlO_3^{3-} = Al_3O_7^{5-} + O^{2-} \qquad K_{12} \quad (9)$$

$$Al_3O_7^{5-} + AlO_3^{3-} = Al_4O_9^{6-} + O^{2-} \qquad K_{13} \quad (10)$$

And finally for a ion chain with n aluminum the polymerization equation could written as:

$$Al_nO_{2n+1}^{(n+2)-} + AlO_3^{3-} = Al_{n+1}O_{2n+3}^{(n+3)-} + O^{2-} \qquad K_{1n} \quad (11)$$

If we assume that:

$K_{11}=K_{12}=K_{13}=\ldots..=K_{1n}$

Then:

$$X_{Al_nO_{2n+1}^{(n+2)-}} = \frac{K_{11}}{X_{O^{2-}}}\left[\frac{1-X_{O^{2-}}}{1-K_{11}\left(1-\frac{1}{X_{O^{2-}}}\right)}\right]^n \quad (12)$$

And:

$$\frac{1}{X_{Al_2O_3}} = \frac{2\,X_{O^{2-}}{}^2\left[\frac{1-X_{O^{2-}}}{1-K_{11}\left(1-\frac{1}{X_{O^{2-}}}\right)}\right]}{K_{11}\,(1-X_{O^{2-}})} + 2(K_{11}-1)\frac{K_{11}{}^2}{X_{O^{2-}}{}^2}\left[\frac{1-X_{O^{2-}}}{1-K_{11}\left(1-\frac{1}{X_{O^{2-}}}\right)}\right] + 4-4K_{11} \quad (13)$$

According to Temkin's theory:

$$a_{MO} = X_{M^{2+}}\,X_{O^{2-}} \quad (14)$$

If we could assume that the concentration of aluminum ions is equal zero, then ($X_{M^{2+}}$=1) and hence:

$$a_{MO} = X_{O^{2-}} \quad (15)$$

And also:

$$\frac{1}{X_{Al_2O_3}} = \frac{2\,a_{MO}{}^2\left[\frac{1-X_{O^{2-}}}{1-K_{11}\left(1-\frac{1}{a_{MO}}\right)}\right]}{K_{11}\,(1-a_{MO})} + 2(K_{11}-1)\frac{K_{11}{}^2}{a_{MO}{}^2}\left[\frac{1-a_{MO}}{1-K_{11}\left(1-\frac{1}{a_{MO}}\right)}\right] + 4-4\,K_{11} \quad (16)$$

Accordingly, the activity of oxide plotted at various equilibrium constants and concentrations has been shown in Figure 2.

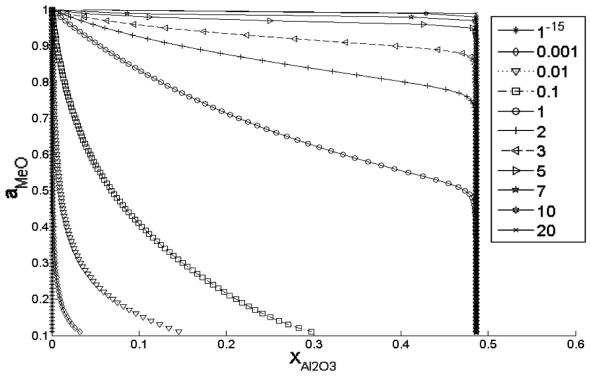


*Fig. 2. Activity of metallic oxide.*

Similarly, according to the present experimental data, the activity of MnO was calculated which has been shown in Figure 3.

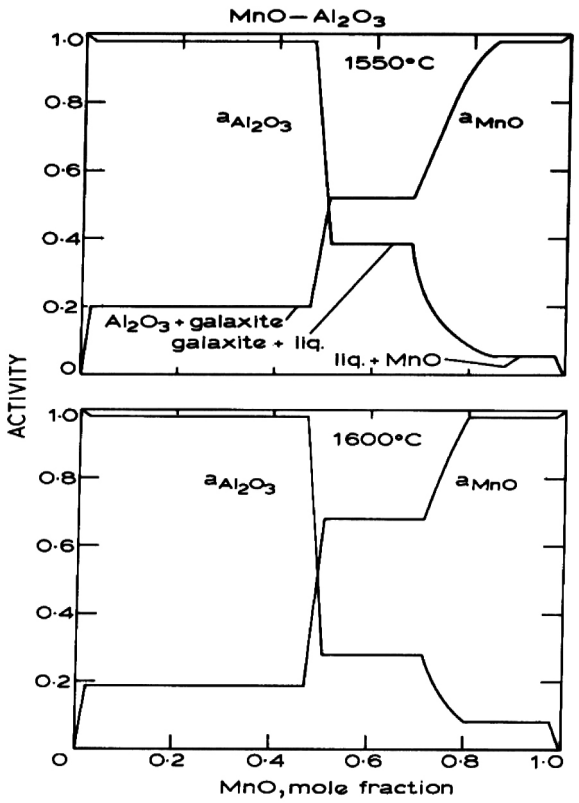


*Fig. 3. Activity of MnO [5].*

Data of Figure 3 was digitized and adjusted with a diagram drawn based on theoretical equations by means of appropriate software. Table 1 shows the equilibrium constant obtained at two specific temperatures.

*Table 1. Variation of the equilibrium constant with temperature*

| K | T (°C) |
|---|---|
| 135 | 1550 |
| 150 | 1600 |

Figure 4 shows the variation of the equilibrium constant vs. temperature. Equilibrium constant value can be determined at different temperatures. ΔG, ΔH and ΔS values can be calculated by thermodynamical relationships. According to the line shown in Figure 4, the relation between constant equilibrium and temperature is as following equation:

$$K = 2.8974e^{0.0021T} \quad (17)$$

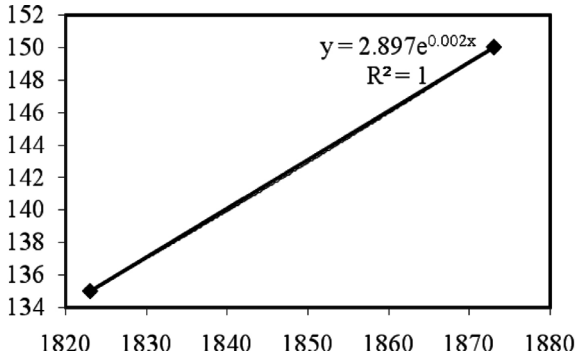


*Fig. 4. Variation of equilibrium constant with temperature.*

**4. Conclusions**

1. An equation was obtained for determining activity in the aluminates melts at the various concentrations of alumina.
2. Theoretical results are in agreement with Experimental results. Hence, the equilibrium constant of MnO was calculated at two temperatures 1550°C and 1600°C.
3. It was determined an exponential ratio between equilibrium constant and temperature.
4. It can be determined ΔG, ΔH and ΔS using the relationship between equilibrium constant and temperature.

**References**

[1] H. S. Ray: Introduction to Melts (Molten Salts & Glasses), Allied Publishers, (2006).
[2] C. Borgianni and P. Granati: Metall. Trans., IOB (1979), 21.
[3] G. W. Toop and V. C. S. Samis: TMS- AIME, 224 (1962), 878.
[4] F. D. Richardson: Physical Chemistry of Melts in Metallurgy, Academic Press, London, (1974).
[5] E. T. Turkdogan: Physicochemical Properties of Molten Slags and Glasses, Metals Society - Technology & Engineering, (1984).
[6] M. M. Mazinan and E. K. Alamdari: Steel Symp. Shahid Chamran Univ., Ahvaz, (1379).
[7] J. J. Moore: Chemical Metallurgy, Second Edition, Butterworths publication company, London, (1990).
[8] C. R. Masson, 1. B. Smith and S. G. Whiteway: Canadian J. Chemistry, 48 (1969), 1456.
[9] W. Y. Yang, W. Cao: Applied numerical methods using MATLAB, John Wiley and Sons, INC, (2005).

International Journal of ISSI, Vol.8 (2011), No.2, pp.27-30

# Failure Analysis of the Openings of Copper Converter in Sarcheshmeh Complex after Service Exposure

M. Mohammadnezhad[1]*, V. Javaheri[2], M. Shamanian[3] and M. Naseri[4]

[1,3] *Department of Materials Engineering, Isfahan University of Technology, Isfahan 84156-83111, Iran.*

[2] *Department of Material Engineering, Iran University of Industries and Mines, Tehran 1439-5518, Iran.*

[2,4] *Research and Development unit of Isfahan Casting Industrial (ICI), Isfahan 83351-11111, Iran.*

## Abstract

In the present study, the austenitic heat resistant cast steel was investigated in as-cast conditions and after being used in copper converter parts. Specimens were cut from an ex-service failed converter part which has been aged for 1900 h. The openings of copper converter in Sarchashmeh Copper Complex in Iran are made of a heat resisting austenitic steel Fe-25Cr-15Ni. Microstructural changes after working period were studied via optical microscopy and scanning electron microscopy equipped with energy dispersive spectrum. The effect of temperature and carbon diffusion on the microstructure, chromium-rich carbides, the chromium carbides transformation to sigma phase and other precipitates during service condition were discussed. The diffusion of $SO_2$ and copper and formation of sub layer decrease the mechanical properties. The formation of sigma phase can be lead to degrade the ductility and toughness.

*Keywords:* Microstructure evolution, Heat resisting steel, Fe-25Cr-15Ni alloy, Fracture mechanism, Sulphidation.

## 1. Introduction

Heat resistant steels are a class of Fe-base alloys that are of interest for their high corrosion and oxidation resistance. They usually contain 12 to 27% Cr and 1 to 2% Mn by (%wt), with the additional Ni in some grades [1]. Also, there is a small amount of carbon in the composition of this steel as an intentional additive or an unavoidable impurity. Heat resistant steels can be classified to three major categories based on the structure: ferritic, martensitic, and austenitic [2].

Cr-Ni austenitic steels are broadly used to make components in mining, metallurgical heat treatment furnace and thermal power generating equipment.

Long-term service at high temperature of austenitic stainless or heat-resistant steels can bring about decomposition of austenite and formation of carbides and intermetallic compounds such as sigma, chi, laves, and epsilon phases [2,3]. Chromium as a basic alloying element is added to iron in order to obtain passivity. It can be added as the amount more than 17% depending on what is required in different environments. In the oxidizing atmosphere, $Cr_2O_3$ surface film is formed. This film is stable up to 1000 ˚C. At higher temperatures $Cr_2O_3$ film volatilizes and transforms to $CrO_3$ which decreases the corrosion resistance of alloys [4].

Heat-resistant Fe-25Cr-15Ni (HH) alloy is the most commonly used cast high temperature furnace compound alloys.

Although heat-resistant austenitic stainless steel castings are designed for use at elevated temperatures, metallurgical degradation can occurs after extended service exposure above 800 ˚C, potentially resulting in embrittlement. The embrittlement is associated with a change in the nature of precipitates at the interdendritic regions of the cast structure during service [5].

In Sarcheshmeh copper complex, the conversion of matte to blister copper is done in a converter and its opening is exposed to 800-1100 ˚C (Figure 1). In this paper, the fracture mechanism of austenitic heat resistant steel was investigated which fails after 1000 hours in copper converter atmosphere.

*Fig. 1. The openings of Sarcheshmeh Copper Converter.*

* *Corresponding author:*
*Tel: +98 311 3802385* *Fax: +98 311 3802384*
*Email: M.mohammadnezhad@ma.iut.ac.ir*
*Address: Department of Materials Engineering, Isfahan University of Technology, Isfahan 84156-83111, Iran.*
*1. M.Sc.*
*2. M.Sc.*
*3. Associate Professor*
*4. M.Sc.*

## 2. Experimental procedure

The alloys used in this study were prepared by induction melting method. Chemical compositions of these alloys have been determined by optical emission spectrometer (OES), as shown in Table 1. In order to produce parts, an induction furnace with acidic lining was used to melt alloys. Then they were cast into a sand mould.

*Table 1. Chemical composition of the alloys, (%wt)*

| | C | Si | Mn | P | S | Cr | Mo | Ni |
|---|---|---|---|---|---|---|---|---|
| Standard | 0.20-0.45 | Max1.75 | Max2 | 0.05 | 0.05 | 23-28 | ---- | 10-14 |
| Casting | 0.25 | 1.8 | 1.06 | 0.024 | 0.005 | 24.7 | 0. 5 | 10.2 |

The working time of parts was 1900 h at 800-1100 ˚C. Test specimens were cut from the as-cast and a section of used parts which have fractured.

Microstructures of alloys were observed using optical microscope (OM) and scanning electron microscope (SEM). Composition analysis and mapping was performed using energy dispersive X-ray spectroscopy (EDX). Metallographic samples (15x15x10 mm) were prepared using 2500-grit paper followed by 1μm diamond polishing. They were etched with marbel etchant (10 gr $CuSo_4$ + 50 ml HCl + 50 ml $H_2O$).

## 3. Results and Discussion

Figure 2 shows the microstructure of alloys in the as-cast state. In this figure, the microstructure comprises austenitic matrix which primary precipitate of carbides are present in grain boundaries and interdendritic areas.

The microstructure of the as-cast samples after 1900 h working time is shown in Figure 3; it can be observed that continuous and thick Cr carbides in grain boundaries.

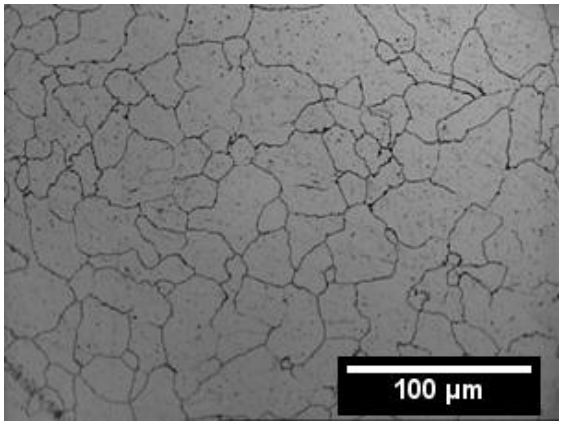


*Fig. 2. Optical microstructure of alloys in the as-cast condition.*

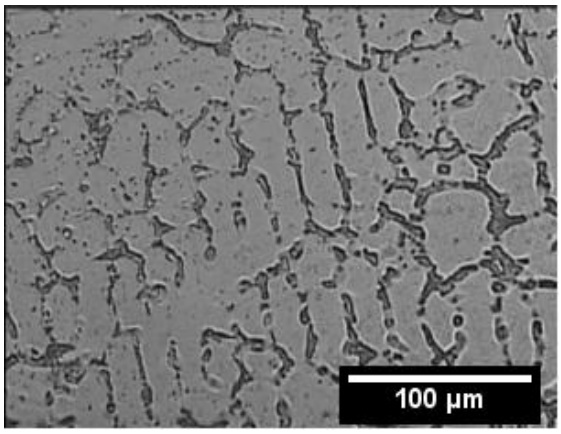


*Fig. 3. Optical microstructure of alloys after working time 1900 h.*

Typically, the Cr carbide is Cr-enriched $M_{23}C_6$ in which M represents Cr and some small amount of Fe. At high temperatures, carbon atoms rapidly diffuse in grain boundaries; so that these atoms can be combined with Cr and they form Cr carbide [6].

Figure 4 shows the SEM micrographs of the long-term service sample. In the as-cast state, eutectic carbides possess an approximately equal area fraction in the austenitic matrix and are separate and distinct from each other in dendrite boundaries. The carbides exhibit a lamellar or skeletal morphology. After service exposure, grain coarsening happened and consequently, the morphology and the area fraction of these eutectic carbides changed.

After working at high temperatures, grain growth, diffusion of carbon in the grain boundaries, coarsening of primary carbides and precipitation of secondary carbides occurred; therefore, impact energy will decreased [5-7].

Austenitic heat resistance steels are entitled to this name due to the presence of primarily austenite in their microstructure. Depending on the balance of ferrite-promoting elements to austenite-promoting elements, the cast microstructure will be either fully austenitic or a mixture of austenite and ferrite. The presence of ferrite in the casting microstructure can degrade the ductility and potentially, the toughness of heat resistance steels. It can also be a preferential site for the precipitation of $M_{23}C_6$ carbides and sigma phase. The latter is an embrittling agent in heat resistance steels [8].

Sigma phase was observed in service-exposed HH alloys using the method outlined in ASTM standard A923. This phase is associated with the Cr-rich constituents in interdendritic sites (Figure 5) and it has been undoubtedly formed during service exposure at Cr-rich regions. The presence of sigma phase in the microstructure can leads to the degradation of ductility and toughness.

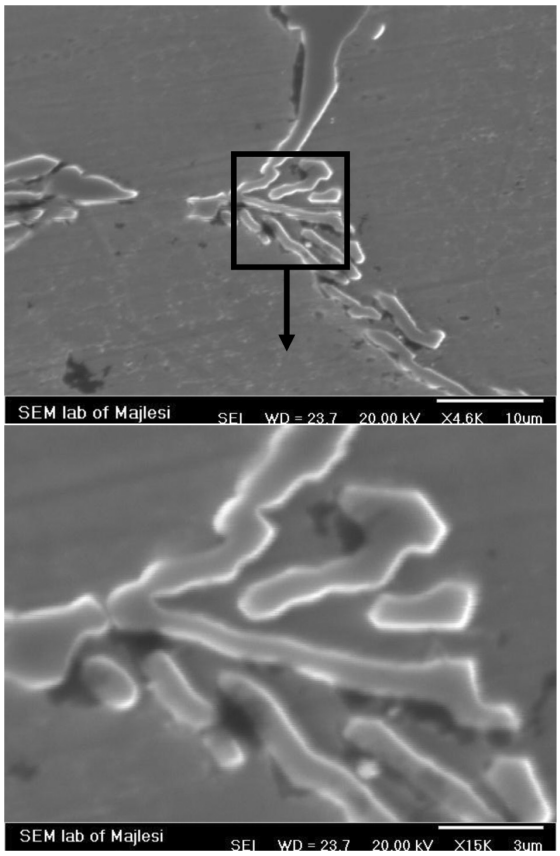


*Fig. 4. SEM micrographs of the used sample austenite and Cr carbide.*

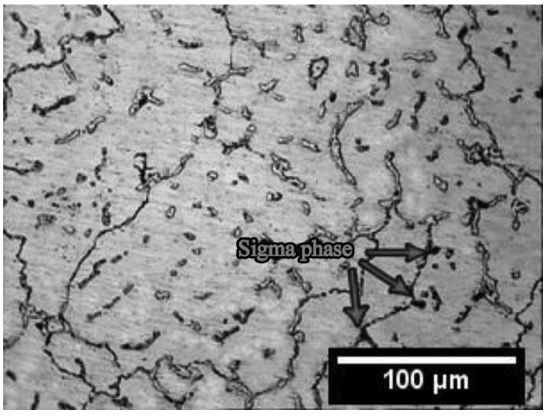


*Fig. 5. Optical micrograph of Sigma phase formed in the microstructure.*

With regard to working condition of parts, several blows are applied to the parts; therefore, decline in impact resistance causes to the fracture of parts.

It was used EDAX in order to composition map analysis. In this technique, various elements are differentiated by identifying each element with distinct color. It is obtained better understanding from the distribution of elements within and around analyzed micro constituents. The elements C, Cr, Fe, Mn, Mo, Ni and Si were chosen for analysis. Figure 6 shows the uniform distribution of the analyzed elements in this alloy in as-cast sample.

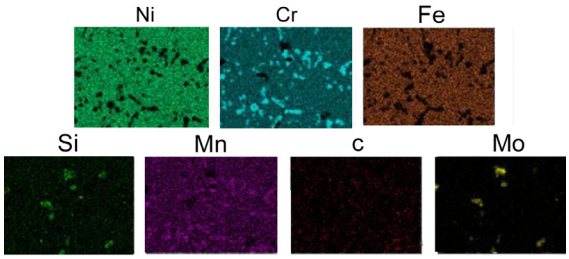


*Fig. 6. X-map analysis of alloy in cast sample.*

Figure 7 shows the microstructure of fracture surface of occurred in the investigated steel and its copper-containing alloys during 1900h service time. Copper contamination cracking (CCC) is a well-known phenomenon in both austenitic stainless steels and heat resistance steels. It occurs in the context of liquid metal embrittlement mechanism; whereby molten copper penetrates in austenite grain boundaries. Since molten copper (or a copper alloy) is a prerequisite in order to occur this mechanism, it can only occur above the melting point of copper, namely 1083°C (1981°F). So, copper wets grain boundaries most effectively at the temperature close to 1100°C. The amount of propagation depends on thermal cycle and applied stress during service time. Residual and/or external stresses tend to accelerate CCC. It will be generally quite straightforward to determine if the cracking mechanism is CCC [9]. As is clear in Figure 7, Copper is observed apparent along austenite grain boundaries due to very distinct color of copper in the microstructure of the steel.

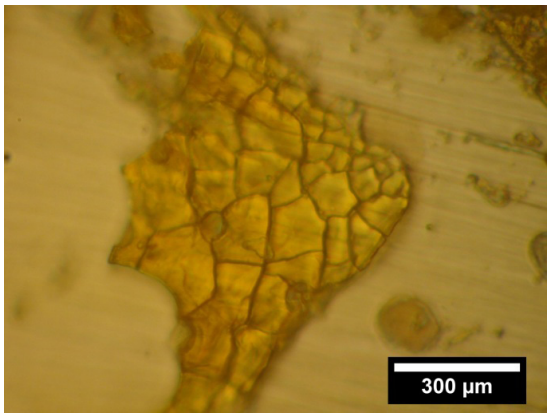


*Fig. 7. The microstructure of fracture surface in the steel and its alloys containing copper after 1900h service time.*

$SO_2$ is another factor which diffuses through pores and micro cracks in the oxide layer; it decomposes and reacts with the surface to form sulfide compounds. Sulphur concentration in grain boundaries causes hot shortness and metal damage (Figure 8). the factors

such as the source of sulphur, effects of stress, and the mode of crack growth which are indicated in the current investigation are consistent with process of the crack tip stress field on the sulphur solute atom; this process is described by "pure drift" model [10-12] in austenitic stainless steels with an F.C.C. structure, it was observed copious internal sulphidation at intermediate sulphur pressures, as predicted for binary alloys with an F.C.C. structure, referred to above.

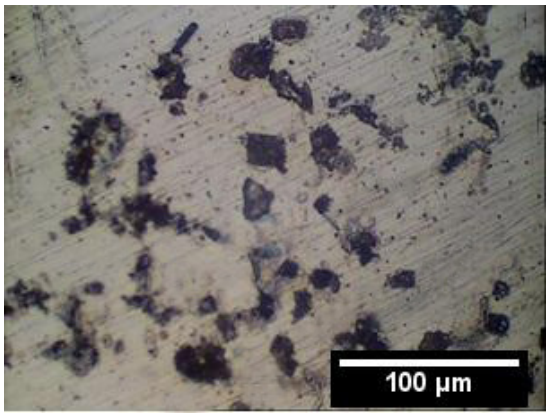


*Fig. 8. The microstructure of fracture surface of steel and its alloys containing sulphides after 1900h service time.*

## 4. Conclusions

Experimental studies on the microstructural evolution and fracture mechanisms of austenitic heat-resistant cast steel Fe-25Cr-15Ni during a long-term service are summarized as follows.

1. The microstructure of the as cast steel consists of dendritic austenite and a small amount of carbide. During service at high temperature for 1900h, continuous and thick Cr carbide formed at grain boundaries.
2. In the service-exposed HH alloys, sigma-phase and Cr-rich $M_{23}C_6$ carbides were present in an austenitic matrix. This matrix contained more than 2% by volume fraction of sigma phase. It can be also expected that this phase to have detrimental effects on mechanical properties and to cause decrease in impact energy.
3. The diffusion of copper and the formation of copper contamination cracking (CCC) decrease mechanical properties and the molten copper penetrates in austenite grain boundaries.
4. High $SO_2$ content in the environment increases the reaction and the formation some spherodized carbides inside grain boundaries itself in both temperatures 900°C–1000°C.

**Acknowledgements**

The authors acknowledge the financial support from Isfahan Casting Industrial (ICI) and are grateful to Senior Engineer Masoud Saba for valuable assistance in carrying out the experiments and valuable comments.

## References

[1] ASM Handbook, Properties and selection: irons, steels, and high performance alloys, Vol. 1, 10th ed., Metals Park, OH 44073, (1990), 908.
[2] T. L. Shinoda, M. B. Zaghloul, Y. Kondo and R. Tanaka: Trans. Iron Steel Inst. Jpn., 18(1998), 139.
[3] M. Karaminezhad, E. Kordzadeh and S. Ebrahimi: Int. J. of ISSI, 2(2005), 31.
[4] S. Jaganathan et al.: Eng. Fail. Anal., 15(2008), 311.
[5] J. Laigo, F. Christien, R. Le Gall, F. Tancret and J. Furtado: Mater. Charact., 59(2008), 1580.
[6] F. G. Imizcoz Caballero, P. Lopez, L. F. Alvarez and C. Andres: Mater. Sci. Technol., 23(2007), 528.
[7] J. M. Gong, S. T. Tu and K. B. Yoon: Eng. Fail. Anal., 6(1999), 143.
[8] M. W. Mucek: Mater. Perform., 9(1983), 25.
[9] L. H. De Almeida, A. F. Ribeiro and I. Le May: Mater. Charact., 49(2002), 219.
[10] B. Piekarski: Mater. Charact., 47(2001), 181.
[11] R. L. Colwell and J. J. Hoffman: Proc. of the NACE int. annual conf. corrosion 98, NACE International, (1998), 423.
[12] E. A. Kenik, P. J. Maziasz, R. W. Swindeman, J. Cervenka and D. May: Scripta Mater., 49(2003), 117.